Stockholm, 28 August 2006

Recent INTEGRAL results

P. Ubertini, Istituto di Astrofisica Spaziale e Fisica Cosmica - Roma

IBIS
15 keV – 10 MeV
FCFOV: 9°x9°
Excellent imaging (12' FWHM), good spectra ≤ E/ΔE~1000

SPI
20 keV – 8 MeV
FCFOV: 16° dia
Excellent spectra (2 keV FWHM @ 1.3 MeV) good images ≤arcmin

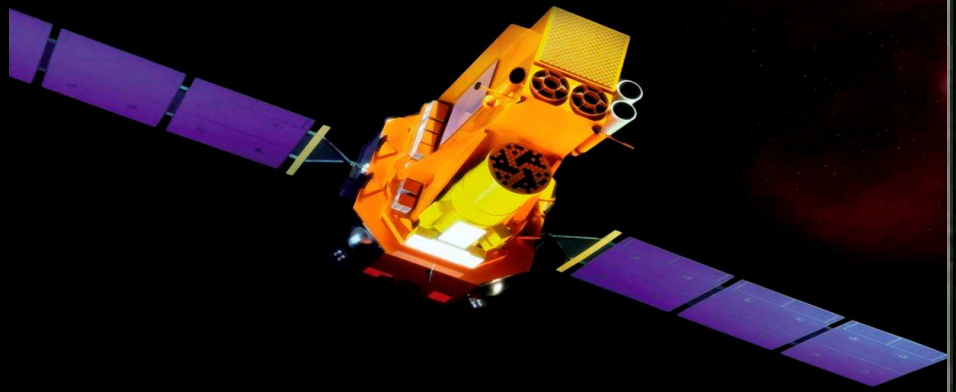

Jem-X
3-35 keV
FCFOV: 4.8°

OMC
500 – 600 nm
FOV: 5°

Coded aperture masks (SPI, IBIS, JEM-X)

IBIS/ISGRI shadowgrams Crab pulsar:
off-axis, on-axis, pulsating (33 ms)

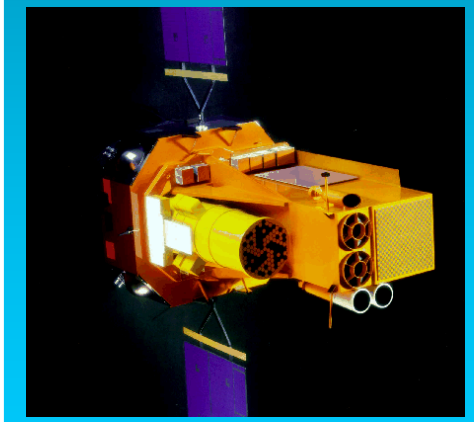

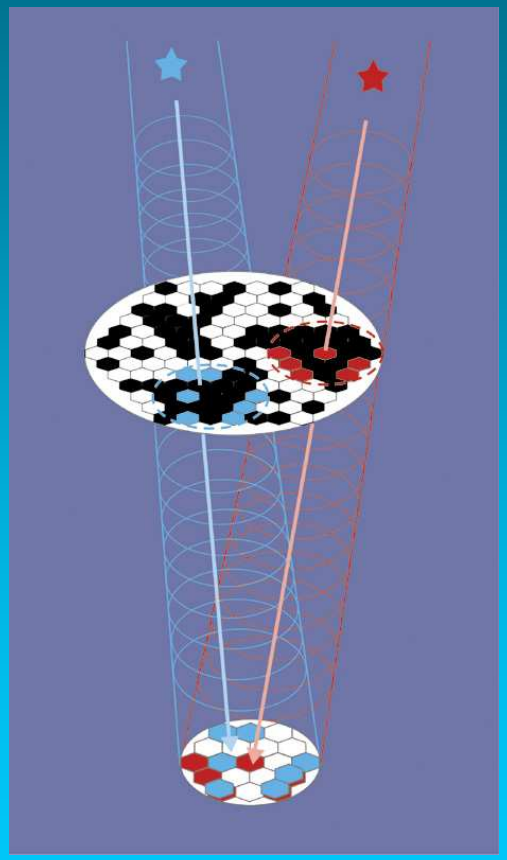

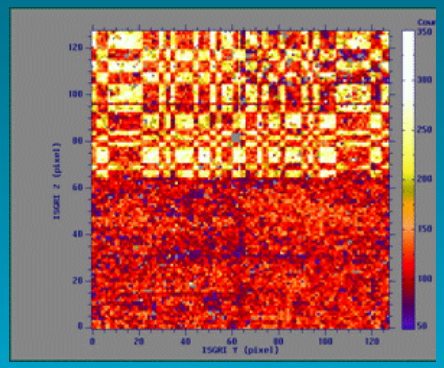

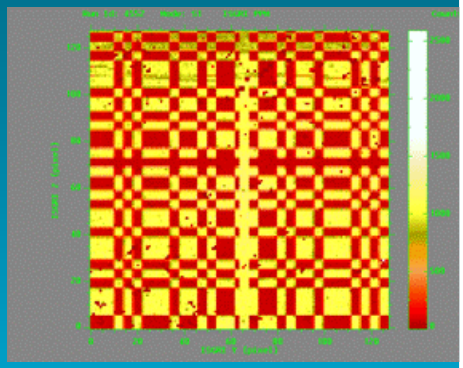

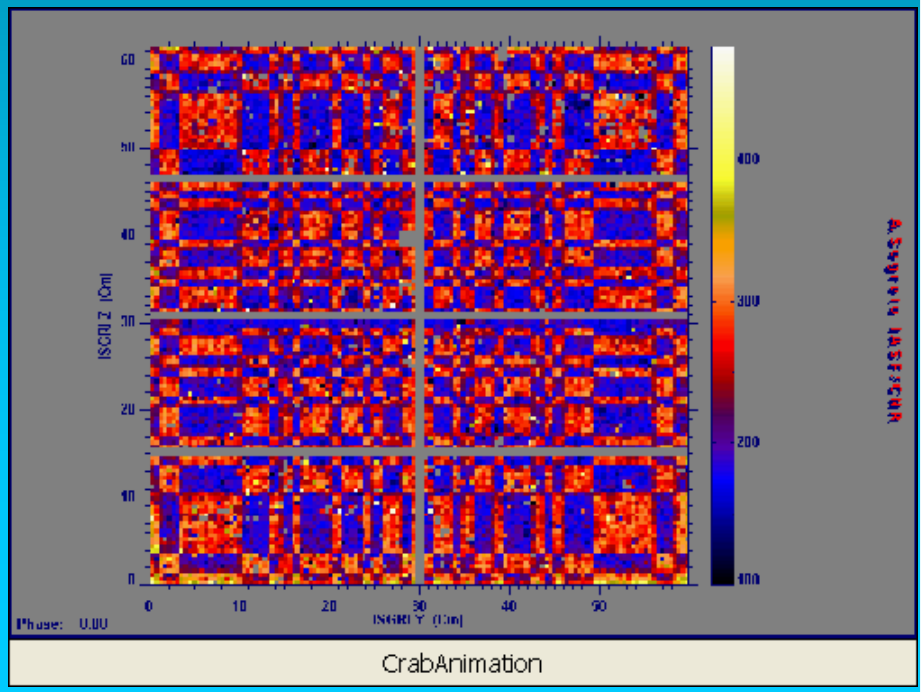

INTEGRAL: coded mask FOV and source multiplicity

Many different source types – outside GC and bulge !

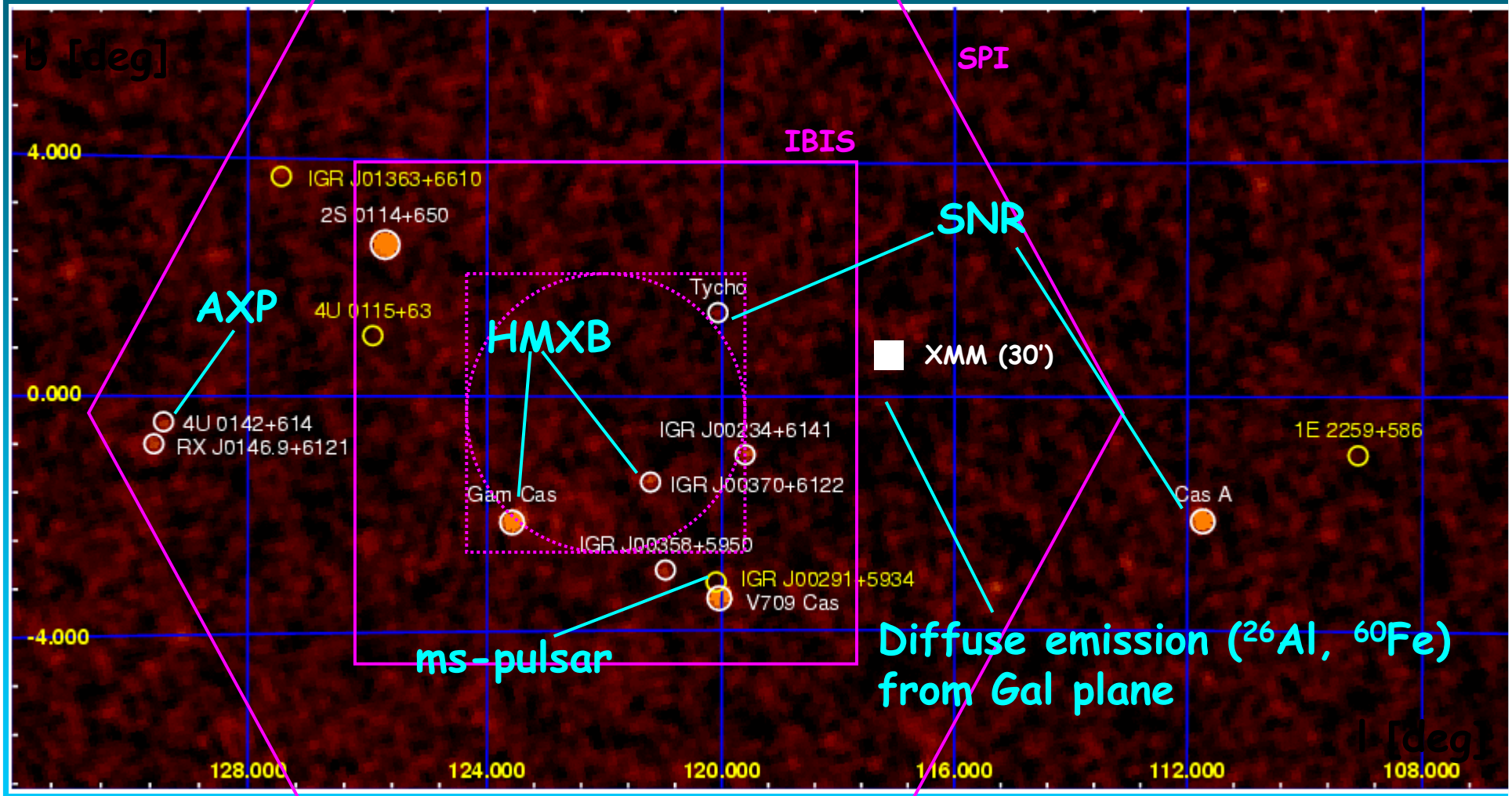

INTEGRAL/IBIS map of Cassiopeia region (20-50 keV)

mosaic 0.7-1.6 Ms, 0.4 – 12 mCrab, den Hartog et al. 2005

2nd Soft γ-ray catalogue A. Bird et al., ApJ, 2006

- 2nd catalogue: 209 sources in **20-100** keV, including
  - Galactic accreting binaries (115)
  - Extragalactic sources (33)
  - 55 IGR's (20% classified)
- Location accuracy:
  40" (10σ), <2' (5σ)
- Limiting sensitivity ~ 1mCrab
- Previous surveys:
  HEAO-1: 14 mCrab
  SIGMA: 30 mCrab

- Expect to finally catalogue > 500 sources (L+5y)

  [HEAO-1/A4 all-sky survey: 72 sources, 13-180 keV, 17 months]

- The gamma ray sky exists!

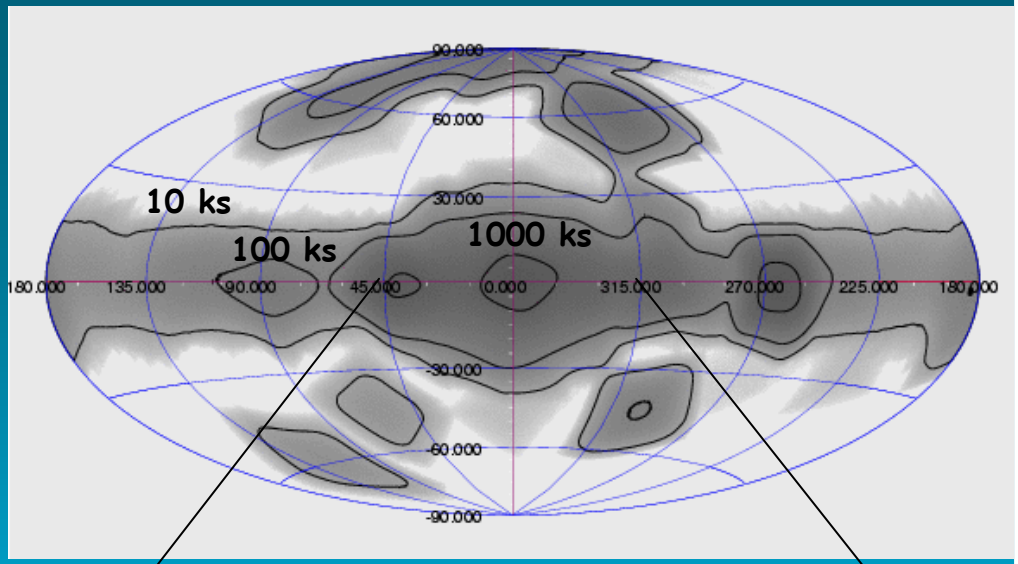

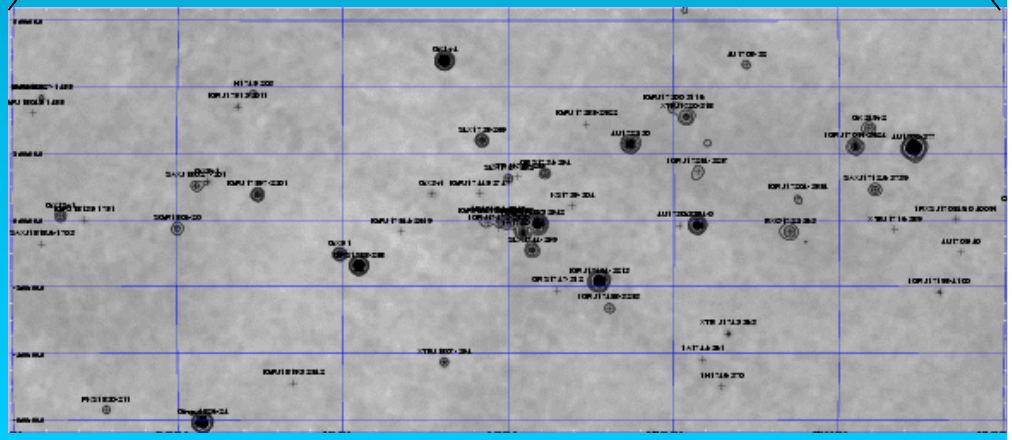

30°

INTEGRAL: advance in imaging

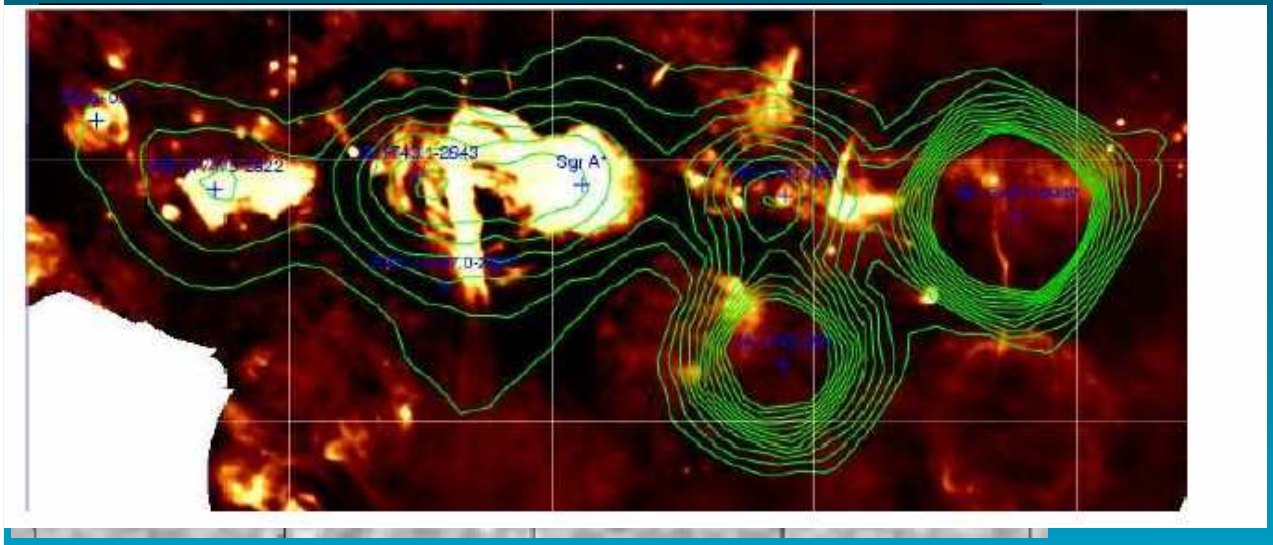

SIGMA, 40-100 keV

Limit. sens: ~ 10 mCrab

Revnivtsev et al., 527, 2004

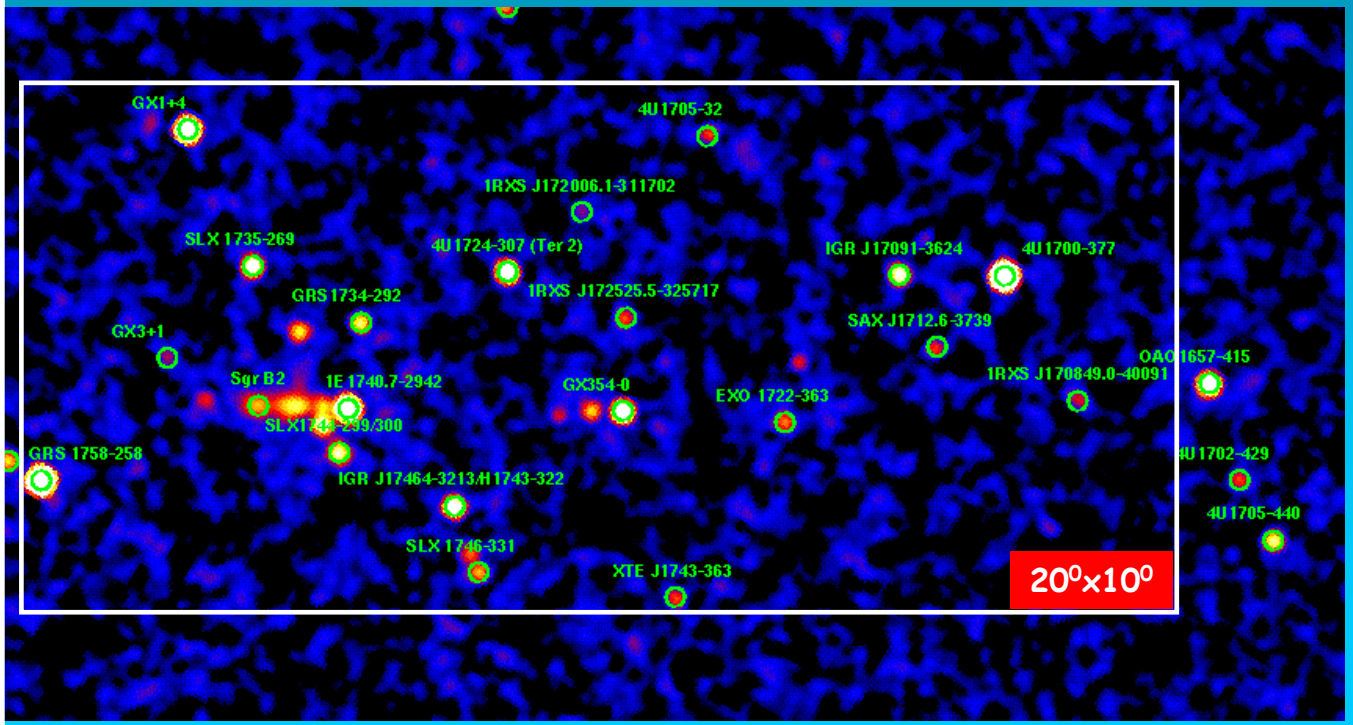

IBIS, 40-130 keV

Limit. sens: 1 mCrab for 1Ms observation (2nd source cat, Bird et al., 2006)

Revnivtsev et al., 2005 (pr comm)

The IBIS soft γ-ray sky

INTEGRAL spatial resolution and improved sensitivity have been key features to solve the numerous point sources of hard X-ray emission detected in particular within the **Galactic centre & Bulge**. Several bright and hard-X-ray flares from SgrA* have been discovered with CHANDRA and XMM opening new perspectives in understanding the process at work in the accreting supermassive black hole of the Galactic centre. At higher energy, the deep INTEGRAL monitoring of this region led to the discovery of emission at E>20 kev in the direction of SgrA complex (IGR J1745.6-2901).
This excess seems to be constant and possibly not associated with the activity of SgrA*. Still need to carefully look for IGR J1745.6-2901 gamma-ray variability when flaring activity is seen in X-ray:

Exposure time **5Ms**

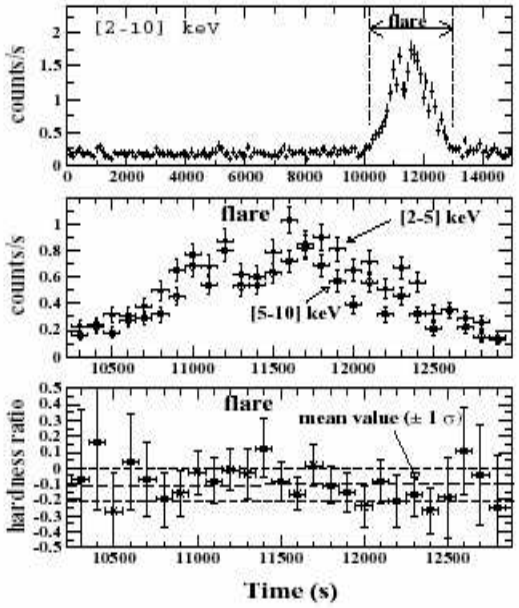

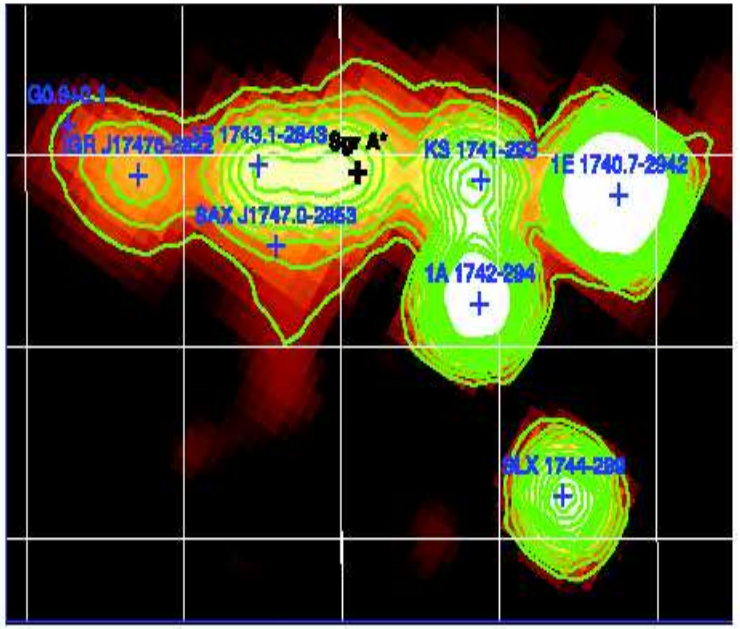

Figure 1: *Left*: Light curves of the very bright X-Ray flare of Sgr A* as observed by XMM-Newton on October 2002 (curves at different energies and hardness ratio). *Right*: Reconstructed sky image in the range 20-40 keV of the central $2° \times 2°$ of our Galaxy obtained from IBIS/ISGRI data collected in about 4.7×10^6 s between 2003 - 2004 with INTEGRAL. A source at the Sgr A* position is detected at the level of 45 σ.

Draft version August 7, 2006
Preprint typeset using LaTeX style emulateapj v. 12/14/05

INTEGRAL/IBIS CENSUS OF THE SKY BEYOND 100 KEV

A. Bazzano[1], J.B. Stephen[2], M. Fiocchi[1], A.J. Bird[3], L. Bassani[2], A.J. Dean[3], A. Malizia[2], P. Ubertini[1], F. Lebrun[4], R. Walter[5] and C. Winkler[6]

Draft version August 7, 2006

ABSTRACT

We report on the first census of INTEGRAL/IBIS detections ($\gtrsim 4\sigma$ significance) above 100 keV based on the Core Program and public Open time observations up to April 2005. There are 49 sources detected in the 100-150 keV band of which 14 are also seen in the 150-300 keV range. The low energy sample is dominated by X-ray binary systems of both low and high mass, but also includes 10 active galaxies. Of the binary systems that are detected above 150 keV, more than 50% are associated with black hole candidates, often reported as microquasars. The present survey results are then used to construct LogN-LogS curves for galactic and extragalactic objects in the 100-150 keV band: above a 1 mCrab sensitivity limit we expect that around 200 galactic sources and almost 350 active galaxies populate the sky above 100 keV. While the contribution of individual point sources to the total Galactic emission has been estimated to be around 70-80% between 100-300 keV, we find that active galaxies detected above 1 mCrab account for only about 3% of the cosmic hard X-ray background in the 100-150 keV band.

Subject headings: surveys — galaxies: active — gamma rays: observations

1. INTRODUCTION

One of the primary goals of the INTEGRAL observatory (39), and in particular of the IBIS imager (38), is to provide a survey of the high energy sky (>20 keV). To this end a number of teams have made an effort to provide a systematic analysis of the data sets, as available to date only, galactic LogN-LogS relation above 100 keV. This was followed by the HEAO 1-A4 survey in the 40-180 keV band (24). Of the 44 sources detected, 14 had a formal statistical significance $\geq 4\sigma$ in the 80-180 keV band, i.e. well above the sensitivity limit of 36 mCrab. The 14 objects detected comprise 6 low mass X-ray bi-

INTEGRAL/IBIS CENSUS OF THE SKY BEYOND 100 KEV

IBIS DETECTIONS IN (100-150)KEV AND (150-300)KEV ENERGY BAND

name	class	IBIS (20-40) keV	IBIS (40-100) keV	IBIS (100-150) keV	IBIS (150-300) keV	SAX (100-150) keV	SAX (150-200) keV	ref
		mCrab	mCrab	mCrab	mCrab	mCrab	mCrab	
4U0142+61	AXP	1.5 ± 0.3	3.4 ± 0.5	8 ± 2				(1)
Crab	PWN PSR	1000.0 ± 0.4	1000.0 ± 0.6	1000 ± 2	1000 ± 6	$1000 \pm 3^{(c)}$	1000 ± 3	
MKN3	AGN	4.2 ± 0.2	6.1 ± 0.4	10 ± 2				
VelaPulsar	PWN PSR	6.74 ± 0.09	8.4 ± 0.1	10.3 ± 0.7				
GS0836-429	LMXB T B	30.58 ± 0.09	27.2 ± 0.1	14.6 ± 0.7				
NGC4151	AGN Sey1.5	32.0 ± 0.6	40 ± 1	35 ± 4		$28.5^{+0.3}_{-0.3}{}^{(b)}$	$18.0^{+0.3}_{-0.5}$	(2)
NGC4388	AGN Sy1	15.9 ± 0.7	17 ± 1	25 ± 5				
3C273	AGN QSO	7.7 ± 0.3	9.2 ± 0.6	12 ± 2		$23.7 \pm 0.7^{(a)}$	27 ± 1	(3)
NGC4507	AGN Sy1h	8.7 ± 0.4	10.7 ± 0.6	10 ± 3				
NGC4945	AGN Sey2	13.2 ± 0.3	20.3 ± 0.4	22 ± 1		$23.1^{+0.6}_{-0.6}{}^{(b)}$		
CenA	AGN Sey2	36.5 ± 0.2	47.4 ± 0.4	57 ± 2	65 ± 6	$49.5^{+0.3}_{-0.3}{}^{(b)}$	$52.0^{+0.5}_{-1.0}$	(4)
Cirgalaxy	AGN Sy1h	13.6 ± 0.2	11.4 ± 0.3	7 ± 1		$3.4^{+1.1}_{-0.5}{}^{(c)}$		
PSRB1509-58	PSR	8.5 ± 0.2	11.0 ± 0.3	14 ± 1				5
XTEJ1550-564	LMXB T BH	70.8 ± 0.2	114.4 ± 0.3	146 ± 1	155 ± 4	$115^{+1}_{-1}{}^{(a)}$	$114.2^{+0.5}_{-1.5}$	(6)
4U1608-522	LMXB T B A	14.3 ± 0.2	7.7 ± 0.3	5 ± 1				
ScoX-1	LMXB Z	629.0 ± 0.4	21.0 ± 0.6	12 ± 2				
4U1630-47	LM							(7)
4U1636-536	L							
OAO1657-415	L							
GX339-4	LI							(8)
4U1700-377								(9)
4U1702-429	L							
4U1705-440	L							
IGRJ17091-3624								(10)
XTEJ1720-318	LM							(11)
GRS1724-30	LM							
GX354-0	L							
GX1+4	L							
SLX1735-269								
1E1740.7-294	L							(12)
KS1741-291	L							
A1742-294	L							
IGRJ17464-3213	L							(13),(14)
SLX1744-299	LMXB B	8.31 ± 0.09	5.4 ± 0.1	4.1 ± 0.5				
IGRJ17597-2201	LMXB B D	7.02 ± 0.09	6.6 ± 0.1	4.3 ± 0.5				
GRS1758-258	LMXB BHC	53.58 ± 0.09	71.6 ± 0.1	78.9 ± 0.5	70 ± 2			(15)
SGRJ1806-20	SGR	3.05 ± 0.09	4.2 ± 0.1	6.8 ± 0.6		$2.4 \pm 0.3^{(a)}$	2.2 ± 0.5	(16)
4U1812-12	LMXB B A	25.6 ± 0.2	26.3 ± 0.3	22 ± 1	18 ± 4			(17)
GS1826-24	LMXB B	79.26 ± 0.09	66.3 ± 0.1	38.2 ± 0.7	12 ± 3	$32.2^{+0.3}_{-0.3}{}^{(b)}$		
PKS1830-211	AGN QSO	2.8 ± 0.2	3.5 ± 0.3	4.4 ± 0.8				(18)
1RX1832-33	LMXB BT G	10.81 ± 0.09	10.9 ± 0.3	8.6 ± 0.8				
KES73	SNR AXP	2.0 ± 0.2	4.0 ± 0.3	6 ± 1		$21 \pm 2^{(a)}$	31 ± 3	
4U1909+07	HMXB T XP	14.3 ± 0.2	9.0 ± 0.3	5.2 ± 0.9				
AqlX1	LMXB BA T	9.6 ± 0.2	5.6 ± 0.3	4.5 ± 0.9		$3.6^{+1.1}_{-0.8}{}^{(a)}$	$3.3^{+1.0}_{-0.6}$	(19)
GRS1915+105	LMXB T BH	260.8 ± 0.2	105.4 ± 0.3	59 ± 1	47 ± 4	$82.6^{+0.2}_{-0.2}{}^{(b)}$	$55.5^{+0.2}_{-0.1}$	(20),(21)
CygX-1	HMXB BH	665.7 ± 0.3	712.5 ± 0.4	632 ± 2	522 ± 6	$950^{+3}_{-3}{}^{(b)}$	870^{+5}_{-5}	(23),(24)
EXO2030+375	HMXB XPBe T	38.8 ± 0.2	20.4 ± 0.4	3.6 ± 0.9				(25)
CygX-3	HMXB	204.1 ± 0.2	85.1 ± 0.3	31 ± 1	20 ± 5	$18.0^{+0.3}_{-0.3}{}^{(b)}$	$12.1^{+0.5}_{-0.5}$	(26)
IGRJ21247+5058	AGNSy 1?	5.6 ± 0.2	7.0 ± 0.4	6.0 ± 1.5				

NOTE. — Class are according with Bird et al. 2006. Beppo-Sax fluxes in millicrab measured by PDS in the band 100-150 and 150-200 k respectivily. Only sources detected with signal to noise maggiore 4 are reported. The notes indicate the model used to fit Beppo-Sax data: (a) simple power law, (b) cut-off power law and (c) broken power law.

They are all known sources

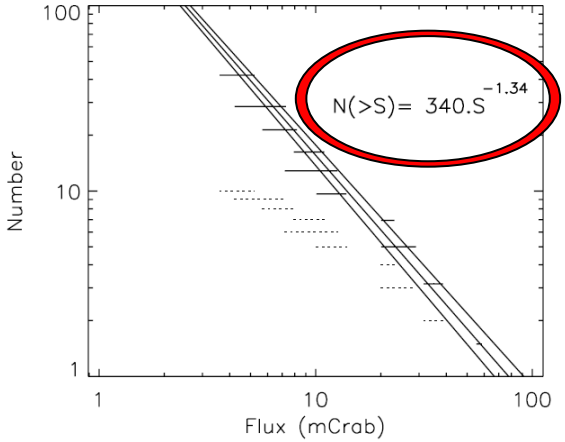

FIG. 4.— The number-flux relationship for the 10 AGN in our sample. Data points for both before (lower, dotted) and after correction for exposure are shown as are the best-fit power law with 1σ limits.

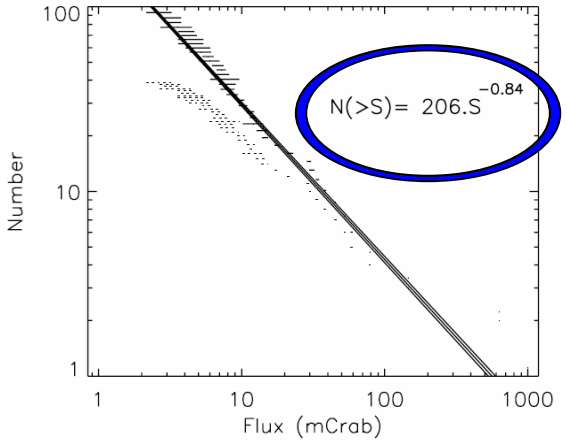

FIG. 5.— As Fig. 4, but for the 39 galactic sources in the sample.

INTEGRAL/IBIS CENSUS OF THE SKY BEYOND 100 KEV

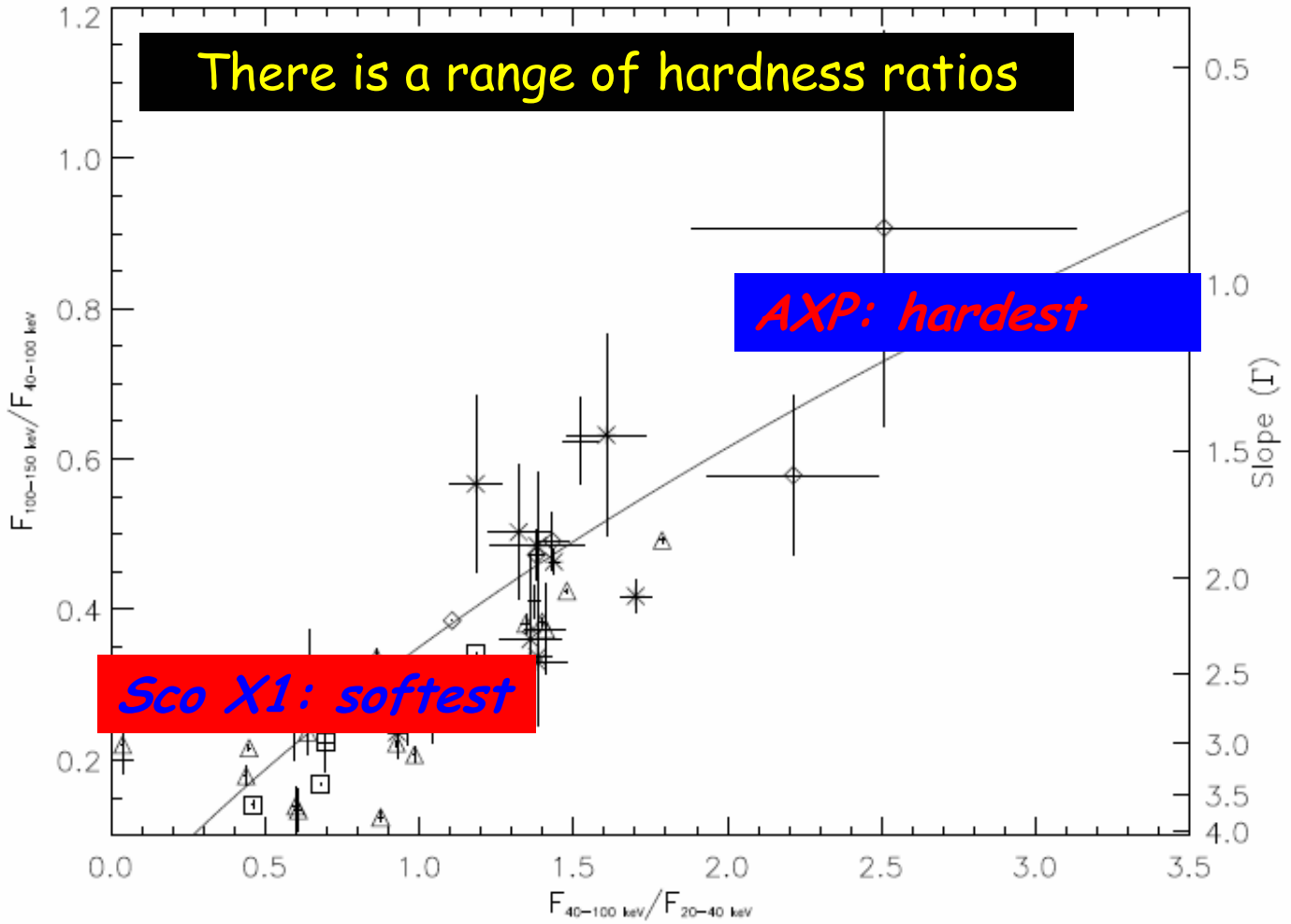

FIG. 1.— The High energy hardness ratio (100-150 keV/40-100 keV) as a function of the low energy hardness ratio (40-100 keV/20-40 keV). The stars are AGN, diamonds are PSR, triangles and squares are LMXB and HMXB and no symbol are unidentified. The curve is the locus of ratios as a function of photon slope (left-hand axis)

The error on the source fux as function of exposure. This relationship is used to compute the flux limit for the entire exposure map.

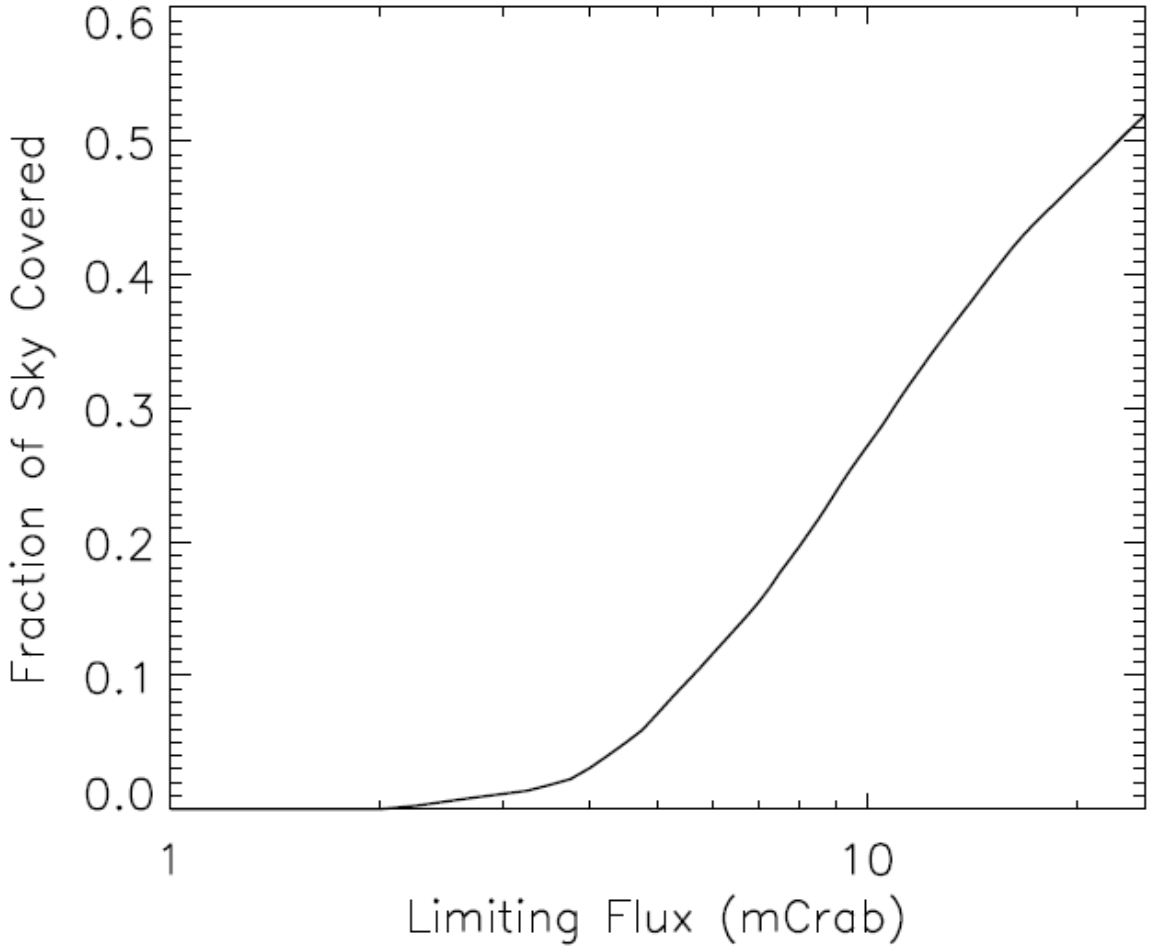

FIG. 3.— The all-sky fractional coverage as a function of (4σ) limiting flux.

x limit for the

All-sky fractional coverage as a function of (4σ) limiting flux.

INTEGRAL observations of the cosmic X-ray background in the

E.Chu
A.Parma
L.E
N.J.We
J.

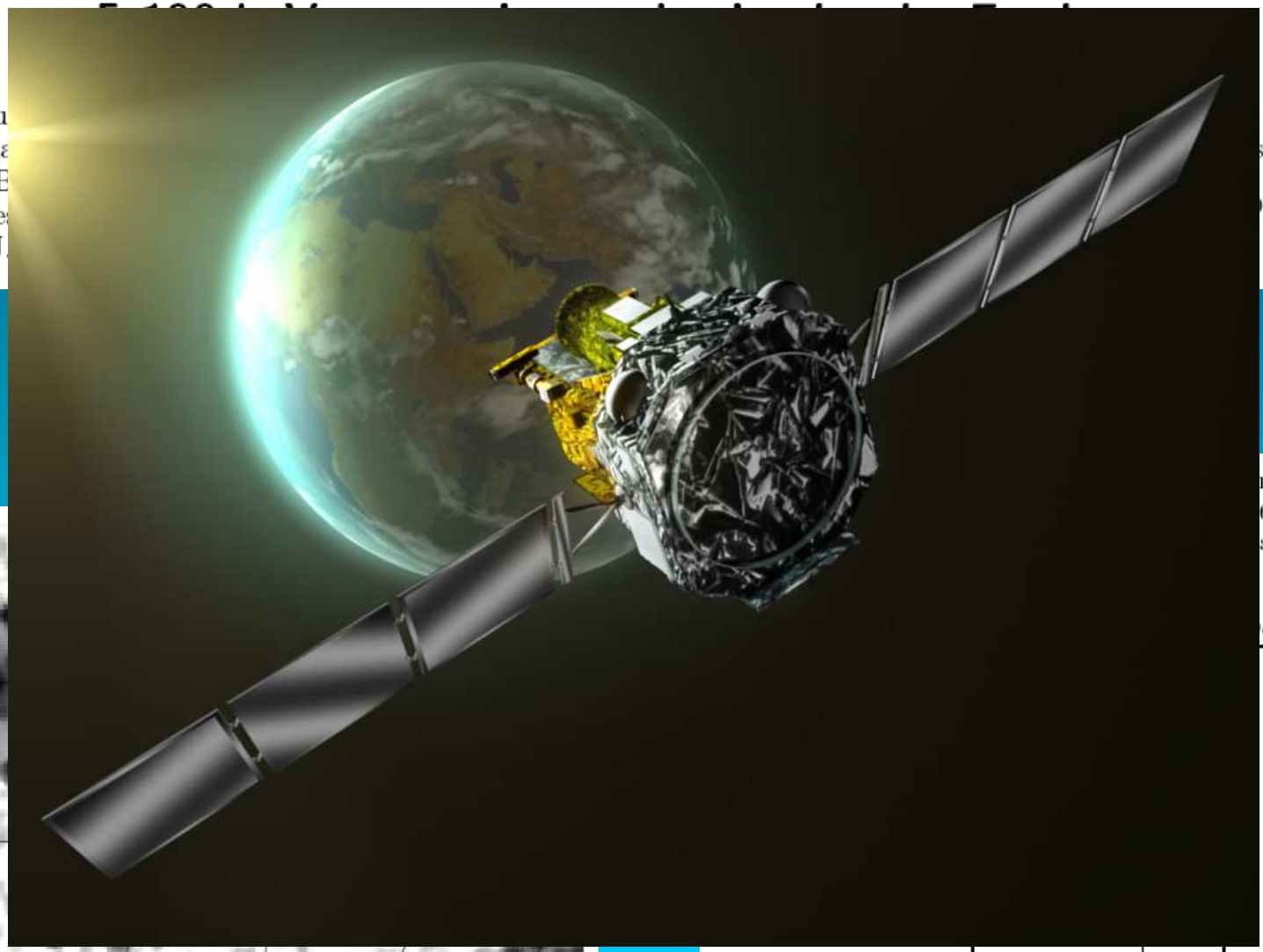

ng the Earth
60 keV band
s discovered

			ccult.
			N
			Y
			Y
			Y
			Y
			Y
			N
			Y
			Y
			Y
XTE J1701-462	15.5 ± 3.3	4.7	N

* - newly detected source

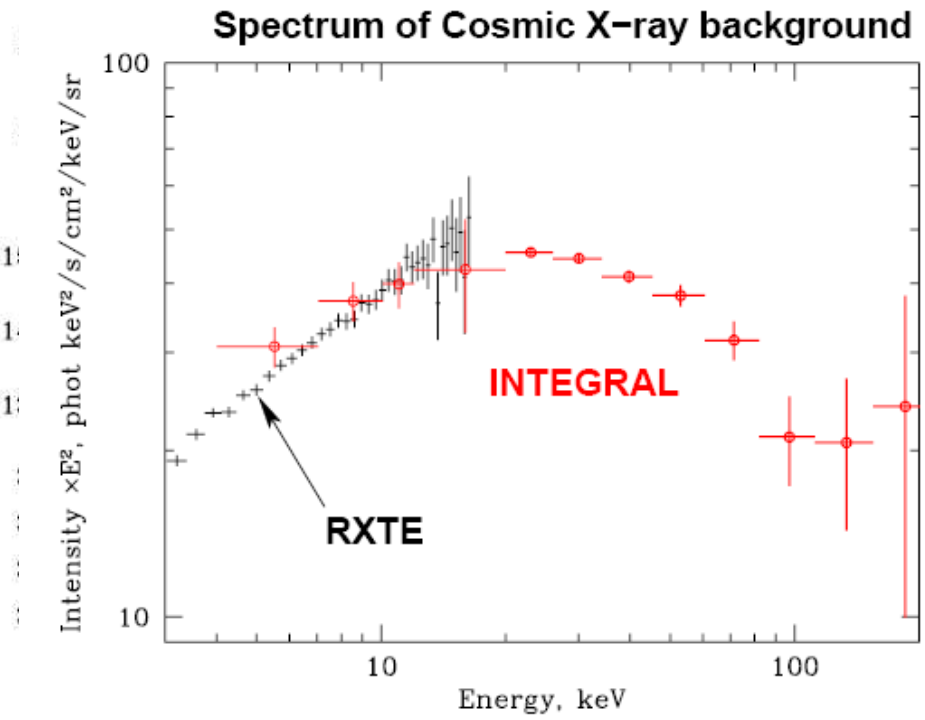

Fig. 12. Comparison of the CXB spectrum derived by INTEGRAL with the 3-20 keV CXB spectrum derived from the RXTE data (Revnivtsev et al. 2003). The IBIS/ISGRI and SPI data points were averaged in this plot.

In Fig.12 we plot the INTEGRAL data together with the CXB spectrum in the 3-20 keV derived from the RXTE data (Revnivtsev et al. 2003). Note that the same reference Crab spectrum was adopted for RXTE analysis. This makes the INTEGRAL/RXTE comparison very straightforward. The normalizations are in a good agreement and are higher than in Gruber et al. (1999). Note that if, instead of the Crab spectrum adopted here, we would use the Crab spectrum adopted in the analysis of HEAO-1/A4 data (see Table 3) the value of the CXB flux in energy band 3 struments would in Gruber et al.

There is room for 10% more flux to explain

5. Conclusions

Using the modulation of the aperture flux by the Earth disk, the INTEGRAL observatory measured the spectrum of the cosmic th X-ray background in the energy range ~5-100 keV. The observed flux near the peak of the CXB spectrum (in the νF_ν units) at 29 keV is 46.9 $keV^2 cm^{-2} s^{-1} keV^{-1} sr^{-1}$. This value is ~10% higher than suggested by Grube et al., 1999. Note that in the preser

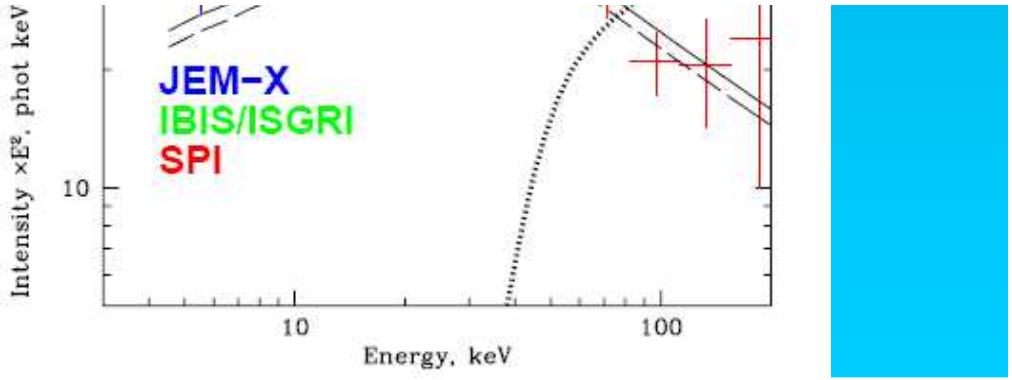

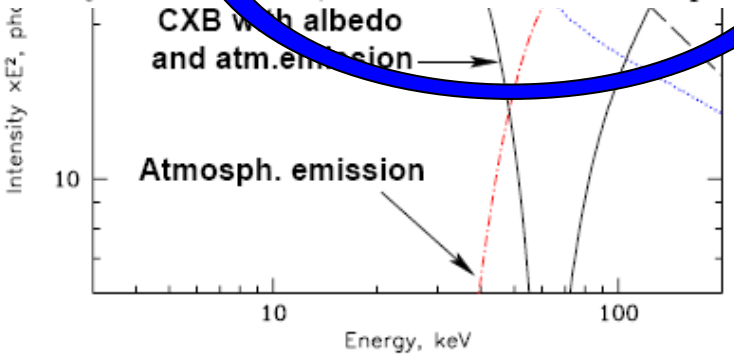

Hard X-ray luminosity function and absorption distribution of nearby AGN: INTEGRAL all-sky survey

S. Sazonov[1,2], M. Revnivtsev[1,2], R. Krivonos[2,1], E. Churazov[1,2], and R. Sunyaev[1,2]

[1] Max-Planck-Institut für Astrophysik, Karl-Schwarzschild-Str. 1, D-85740 Garching bei München, Germany
[2] Space Research Institute, Russian Academy of Sciences, Profsoyuznaya 84/32, 117997 Moscow, Russia

Received / Accepted

ABSTRACT

Aims. We study the hard X-ray luminosity function and absorption distribution of local ($z \lesssim 0.1$) active galactic nuclei (AGN), and discuss the implications for AGN cosmological evolution and for the cosmic X-ray background (CXB).

Methods. We use the INTEGRAL all-sky hard X-ray survey to perform a statistical study of a representative sample of nearby AGN. Our entire all-sky sample consists of 123 AGN, of which 91 are confidently detected ($> 5\sigma$) on the time-averaged map obtained with the IBIS/ISGRI instrument and 32 are detected only during single observations. Among the former there are 66 non-blazar AGN located at $|b| > 5^\circ$, where the survey's identification completeness is $\sim 93\%$, which we use for the calculation of the AGN luminosity function and X-ray absorption distribution.

Results. In broad agreement with previous studies, we find that the fraction $f_{\rm a}$ of obscured ($\log N_{\rm H} > 22$) objects is much higher ($\sim 70\%$) among the low-luminosity AGN ($L_{\rm hx} < 10^{43.6}$ erg s^{-1}) than among the high-luminosity ones ($L_{\rm hx} > 10^{43.6}$ erg s^{-1}), $f_{\rm a} \sim 25\%$, where $L_{\rm hx}$ is the luminosity in the 17–60 keV energy band. We also find that locally the fraction of Compton-thick AGN is less than 20% unless there is a significant population of so strongly obscured AGN that their observed hard X-ray luminosities fall below $\sim 10^{40}$–10^{41} erg s^{-1}, the effective limit of our survey. The constructed hard X-ray luminosity function has a canonical smoothly connected two power-law shape in the range $40 < \log L_{\rm hx} < 45.5$ with a characteristic luminosity of $\log L_* = 43.40 \pm 0.28$. The estimated local luminosity density due to AGN with $\log L_{\rm hx} > 40$ is $(1.4 \pm 0.3) \times 10^{39}$ erg s^{-1} Mpc^{-3} (17–60 keV). We demonstrate that the spectral shape and amplitude of the CXB can be explained in the simple scenario in which at all redshifts for a given $L_{\rm hx}/L_*(z)$ the $N_{\rm H}$ distribution of AGN is similar to that measured by INTEGRAL at $z \lesssim 0.1$ while the AGN luminosity function experiences pure luminosity evolution as suggested by deep extragalactic X-ray surveys.

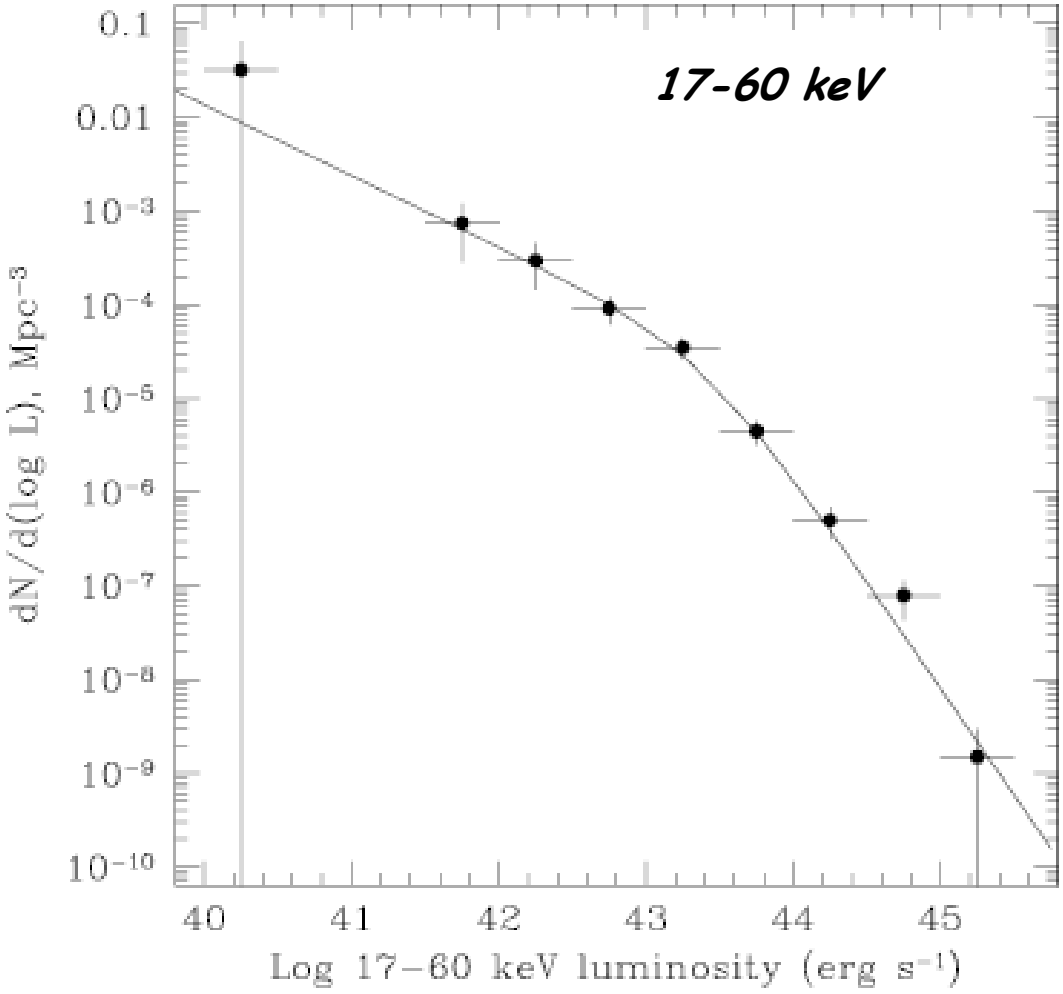

Fig. 4. Hard X-ray luminosity function of local emission-line AGN obtained with INTEGRAL in binned form (solid circles and 1σ error bars). The solid line shows the analytic approximation given by equation (1) and Table 3.

One of the most surprising results of the survey is that very few Compton-thick AGN have been detected, all of them having been known before. The observed fraction of Compton-thick objects is only $\sim$ 10%. This estimate may increase to at most $\sim$ 20% once the currently missing absorption columns are measured. Clearly Compton-thick AGN are fairly rare. A note of caution is necessary here concerning very Compton-thick objects ($\log N_{\rm H} \sim 25$–26). Since their observed hard X-ray luminosities are expected to be $\lesssim$ 10% of their intrinsic luminosities, such sources may constitute a major fraction of AGN at luminosities near our survey's effective limit ($L_{\rm hx} \sim 10^{40}$–10^{41} erg s^{-1}) and below.

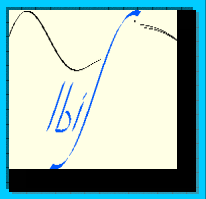

Next steps

- Fully understand the CXB results in term of AGNs distribution/ models (Compton thin vs thick, Blazars etc, luminosity function …
- Complete the Galaxy plane survey (AO5)
- Expand the all sky coverage (Integral to observe till december 2009)
- Fully implement the "key program" scheme (GLAST inputs?, 17 Nov dead line)
- Improve coordinated observation with SWIFT, RXTE, XMM & CHANDRA (Sakuko?)

and finally

- Continue the (ongoing) strong optical,IR, Radio counterpart identification programme (that will also be relevant for GLAST)

Microquasars detected at hard X-ray/TeV energies

LS 5039

Associated with **HESS J1826-148**

(Aharonian et al. 2005, Science, 309)

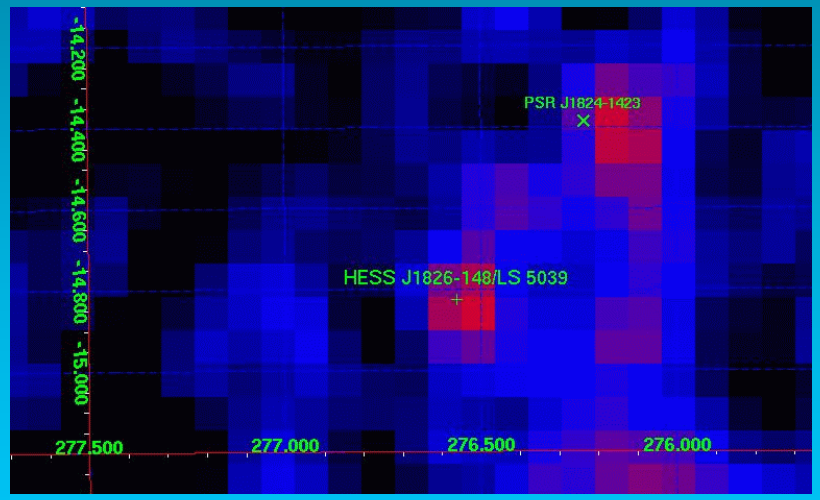

IBIS/ISGRI 20-100 keV mosaic of ~900 Ks centered on LS 5039. The microquasar has been detected at more than 6σ level.

LS +61 303

detected by **MAGIC**

(Albert et al. 2006, astro-ph/0605549)

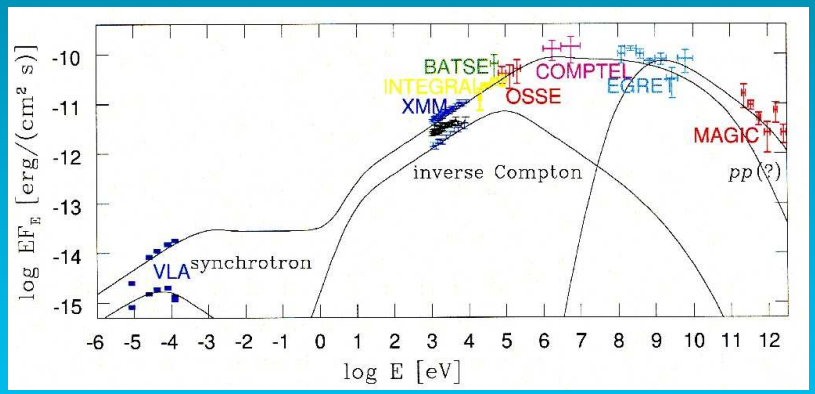

Broad band spectrum of LS +61 303 as reported by Chernyakova et al.2006.

Yellow points are the IBIS/ISGRI average spectrum from Jan 2003 to Mar 2005.